

1 **Bias in estimated short sprint profiles using timing gates due to the**
2 **flying start: simulation study and proposed solutions¹**

3 Mladen Jovanović

4 *Faculty of sport and physical education*

5 *University of Belgrade, Serbia*

6 ORCID: 0000-0002-4013-6530

7 coach.mladen.jovanovic@gmail.com

8 Twitter: @physical_prep

9 Short sprints are most frequently evaluated and modeled using timing gates. Flying start distance is
10 often recommended to avoid premature timing system triggering by lifting knees or swinging arms.
11 This results in timing system initiation not being aligned with the initial force application, which
12 yields bias in estimated short sprint parameters. This simulation study aims to explore the effects of
13 the flying start distance on bias and sensitivity to detect changes in short sprint parameters using
14 three models: the contemporary No Correction model and two proposed Estimated time correction
15 (Estimated TC), and Estimated flying distance (Estimated FD) models. In conclusion, both the
16 Estimated TC and Estimated FD models provided more precise parameter estimates, but
17 surprisingly, the No correction model provided higher sensitivity for specific parameter changes.
18 Besides standardizing the sprint starting technique for the short sprint performance monitoring,
19 practitioners are recommended to utilize and track the results of all three models.

20 **Keywords:** acceleration, error, profile, velocity, model

¹ This is an Accepted Manuscript of an article published by Taylor & Francis in *Computer Methods in Biomechanics and Biomedical Engineering* on 28 Jan 2023, available at: <http://www.tandfonline.com/10.1080/10255842.2023.2170713>

21 **Introduction**

22 Sprint speed is one of the most distinctive and admired physical characteristics in
23 sports. In most team sports (e.g., soccer, field hockey, handball, etc.), short sprints are
24 defined as maximal sprinting from a standstill across a distance that does not result in
25 deceleration at the finish. Peak anaerobic power is reached during the first few seconds
26 (<5 s) of maximal efforts (Mangine et al. 2014); however, the capacity to attain
27 maximal sprint speed is athlete- and sport-specific. For instance, track and field
28 sprinters are trained to achieve maximal speed later in a race (i.e., 50-60 m) (Ward-
29 Smith 2001), whereas team sport athletes have sport-specific attributes and reach
30 maximal speed much earlier (i.e., 30-40 m) (Brown et al. 2004). The evaluation of short
31 sprint performance is frequently included in a battery of fitness tests for various sports,
32 regardless of the kinematic differences between athletes.

33 The use of force plates is regarded as the gold standard for analyzing the mechanical
34 features of sprinting; nevertheless, collecting the profile of a whole sprint presents
35 practical and cost problems (Samozino et al. 2016; Morin et al. 2019). Radar and laser
36 technology are frequently utilized laboratory-grade methods (Buchheit et al. 2014;
37 Jiménez-Reyes et al. 2018; Marcote-Pequeño et al. 2019; Edwards et al. 2020) that are
38 typically unavailable to sports practitioners. Timing gates are unquestionably the most
39 prevalent method available for modeling and evaluating sprint performance. Multiple
40 gates are placed at different distances to capture split times (e.g., 10, 20, 30, and 40 m),
41 which can now be incorporated into the method for determining sprint mechanical
42 properties (Samozino et al. 2016; Morin et al. 2019). Practitioners can utilize the
43 outcomes to explain individual differences, quantify the effects of training
44 interventions, and gain a better knowledge of the limiting variables of performance.

45

46 To ensure accurate short sprint parameter estimates using timing gates, the initial force
47 production must be synced with start time, often referred to as “first movement”
48 triggering (Haugen et al. 2012; Haugen and Buchheit 2016; Samozino et al. 2016;
49 Haugen et al. 2019; Haugen, Breitschädel, and Seiler 2020; Haugen, Breitschädel, and
50 Samozino 2020). This represents a challenge when collecting sprint data using timing
51 gates and can substantially impact estimated parameters. From a measurement
52 perspective, *flying start* distance is often recommended to avoid premature triggering of
53 the timing system by lifted knees or swinging arms (Altmann et al. 2015; Haugen and
54 Buchheit 2016; Altmann et al. 2017; Altmann et al. 2018; Haugen, Breitschädel, and
55 Samozino 2020). Flying start can also result from body rocking during the standing
56 start. Clearly, any flying start with a difference between the initial force production and
57 the start time can lead to bias in estimated short sprint parameters. Since it is hard to get
58 faster at a sprint, inconsistent starts can hide the effects of the training intervention.
59 This work aims to explore the bias and sensitivity to detect changes due to flying start
60 involved when estimating short sprint parameters under simulated conditions. In
61 addition, two novel model definitions are proposed with the aim of minimizing the
62 parameter bias and increasing sensitivity to detect changes. This is needed to provide a
63 theoretical understanding of the limits and expected errors of the short sprints modeling,
64 which can later inform more practical studies involving athletes.

65 **Methods**

66 *Mathematical model*

67 The mono-exponential Equation 1 has been used to model short sprints. It was first
68 proposed by Furusawa et al. (1927) and made more popular by Clark et al. (2017) and
69 Samozino et al. (2016). Equation 1 is the function for instantaneous horizontal velocity

70 v given time t and two model parameters: (1) *Maximum sprinting speed* (MSS;
71 expressed in ms^{-1}) and (2) *relative acceleration* (TAU; expressed in s).

$$72 \quad v(t) = MSS \times \left(1 - e^{-\frac{t}{TAU}}\right) \quad (1)$$

73 TAU represents the ratio of MSS to initial acceleration (MAC; *maximal acceleration*,
74 expressed in ms^{-2}) (Equation 2). Note that TAU, given Equation 1, can be interpreted
75 as the time required to reach a velocity equal to 63.2% of MSS.

$$76 \quad MAC = \frac{MSS}{TAU} \quad (2)$$

77 Although TAU is utilized in the equations and afterward estimated, it is preferable to
78 use and report MAC because it is simpler to understand, especially for practitioners and
79 coaches. By deriving Equation 1, Equation 3 is obtained for horizontal acceleration.

$$80 \quad a(t) = \frac{MSS}{TAU} \times e^{-\frac{t}{TAU}} \quad (3)$$

81 By integrating Equation 1, the equation for distance covered (Equation 4) is obtained.

$$82 \quad d(t) = MSS \times \left(t + TAU \times e^{-\frac{t}{TAU}}\right) - MSS \times TAU \quad (4)$$

83 ***Model parameters estimation using timing gates split times***

84 Table 1 contains sample split times measured during 40 m sprint performance using
85 timing gates positioned at 5, 10, 20, 30, and 40 m.

86

87 **[Insert Table 1 here]**

88

89 To estimate model parameters using split times, distance is a *predictor*, and time is the
90 *outcome* variable; hence, Equation 4 takes the form of Equation 5 (Vescovi and
91 Jovanović 2021; Jovanović and Vescovi 2022).

92
$$t(d) = TAU \times W \left(-e^{\frac{-d}{MSS \times TAU}} - 1 \right) + \frac{d}{MSS} + TAU \quad (5)$$

93 W in Equation 5 represents *Lambert's W* function, which is defined to be the
94 multivalued inverse of the function $f(w) = we^w$ (Corless et al. 1996; Goerg 2022).
95 Equation 4, in which time is the predictor and distance is the outcome variable, is
96 commonly employed in research (Morin 2017; Morin and Samozino 2019; Stenroth and
97 Vartiainen 2020). This method should be avoided since reversing the predictor and
98 outcome variables in a regression model may create biased estimated parameters
99 (Motulsky 2018, p. 341). This bias may not be practically significant for profiling short
100 sprints, but it is a statistically flawed practice and should be avoided. It is thus
101 preferable to utilize statistically correct Equation 5 to estimate model MSS and TAU.
102 Estimating MSS and TAU parameters using Equation 5 as the model definition is
103 performed using *non-linear least squares regression*. To the best of my knowledge,
104 scientists, researchers, and coaches have been performing short sprints modeling using
105 the built-in solver function of Microsoft Excel (Microsoft Corporation, Redmond,
106 Washington, United States) (Samozino et al. 2016; Clark et al. 2017; Morin 2017;
107 Morin et al. 2019; Stenroth et al. 2020; Stenroth and Vartiainen 2020). These, and
108 additional functionalities, have been recently implemented in the open-source **{shorts}**
109 package (Vescovi and Jovanović 2021; Jovanović 2022; Jovanović and Vescovi 2022)
110 for R-language (R Core Team 2022), which utilizes the *nlsLM()* function from the
111 **{minpack.lm}** package (Elzhov et al. 2022). Compared to the built-in solver function of
112 Microsoft Excel, the **{shorts}** package represents a more feature-rich, flexible,
113 transparent, and reproducible environment for modeling short sprints. It is used in this
114 study to estimate model parameters.
115 Using the split times from Table 1, estimated MSS, TAU, and MAC parameters equal to
116 9.02 ms^{-1} , 1.14 s , and 7.94 ms^{-2} , respectively. *Maximal relative power* (P_{MAX};

117 expressed in W/kg) is an additional parameter often estimated and reported (Samozino
118 et al. 2016; Morin et al. 2019). P_{MAX} is calculated using Equation 6. This method of
119 P_{MAX} estimation disregards the air resistance and thus represents *net* or relative
120 *propulsive* maximal power. Calculated P_{MAX} using estimated MSS and MAC
121 parameters equal to 17.91 W/kg .

$$122 \quad P_{MAX} = \frac{MSS \times MAC}{4} \quad (6)$$

123 ***Problems with parameters estimation using split times due to flying start and***
124 ***reaction time***

125 To demonstrate impact of the flying start and reaction time on estimated parameters,
126 imagine three hypothetical triplet brothers, Mike, Phil, and John, with the same short
127 sprint characteristics: MSS equal to 9 ms^{-1} , TAU equal to 1.125 s, MAC equal to 8
128 ms^{-2} , and P_{MAX} equal to 18 W/kg (these represent *true* short sprint parameters).
129 They all performed a 40 m sprint from a standing start using timing gates positioned at
130 5, 10, 20, 30, and 40 m. For Mike and Phil, the timing system is activated by the initial
131 timing gate (i.e., when they cross the beam) at the start of the sprint (i.e., $d = 0$ m). For
132 John, the timing system is activated after the gunfire.
133 Mike represents the *theoretical model*, in which it is assumed that the initial force
134 production and the timing initiation are perfectly synchronized. Mike's split have
135 already been enlisted in Table 1. Phil decided to move slightly behind the initial timing
136 gate (i.e., for 0.5 m) and used body rocking to initiate the sprint start. In other words,
137 Phil used a *flying start*, a common scenario when testing field sports athletes. Since the
138 gunfire triggers John's start, his split times have an additional reaction time of 0.2 s.
139 This is similar to a scenario where the athlete prematurely triggers a timing system

140 when standing too close to the initial timing gate. John's data can thus be used to
141 demonstrate the effects of this scenario on the estimated parameters.
142 Timing gates utilized in this theoretical example provide precision to two decimals (i.e.,
143 closest 10 *ms*), representing a measurement error source. A graphical representation of
144 the sprint splits can be found in Figure 1.

145

146 **[Insert Figure 1 here]**

147

148 Estimated sprint parameters can be found in Table 2. As seen from the results (Table 2),
149 estimated short sprint parameters for all three brothers differ from the *true* parameters
150 used to generate the data (i.e., their *true* short sprint characteristics). All three brothers
151 have a bias in estimated parameters due to timing gates' precision to 2 decimals (i.e., 10
152 *ms*). Bias in estimated parameters in Phil's case is due to the flying start involved,
153 while in John's case, it is due to the reaction time involved in the split times.

154

155 **[Insert Table 2 here]**

156 ***How to overcome missing the initial force production when using timing gates?***

157 The literature suggests using a correction factor of +0.5 s as a viable solution (i.e.,
158 simply adding +0.5 s to split times) to convert to "first movement" triggering when
159 utilizing recommended 0.5 m flying distance behind the initial timing gate (Haugen et
160 al. 2012; Haugen and Buchheit 2016; Haugen et al. 2019; Haugen, Breitschädel, and
161 Seiler 2020). Intriguingly, the average difference between the standing start with a
162 photocell trigger and a block start to gunfire for a 40-meter sprint was 0.27 s (Haugen et
163 al. 2012). Consequently, although a timing correction factor is required to prevent

164 further inaccuracies in estimates of kinetic variables (e.g., overestimate power), a
165 correction factor that is too big would have the opposite effect (e.g., underestimate
166 power).

167 *The Estimated time correction model*

168 Instead of using *a priori* time correction from the literature, this parameter may be
169 estimated using the supplied data, together with MSS and TAU. Stenroth et al. (2020)
170 propose the same approach, titled the *time shift method*, and the estimated parameter,
171 named the *time shift parameter*. In accordance with the current literature, this parameter
172 is termed *time correction* (TC) (Vescovi and Jovanović 2021).
173 Using the original Equation 5 to implement the TC parameter now yields the new
174 Equation 7. Equation 7 is utilized as the model definition in the *Estimated TC* model, as
175 opposed to the model using Equation 5, which is termed the *No correction* model in this
176 study. The model in which TC is fixed (i.e., by simply adding TC to split times) is
177 termed the *Fixed TC* model.

$$178 \quad t(d) = TAU \times W \left(-e^{\frac{-d}{MSS \times TAU}} - 1 \right) + \frac{d}{MSS} + TAU - TC \quad (7)$$

179 From a regression perspective, the TC parameter can be viewed as an *intercept*. It can
180 be beneficial when assuming a fixed time shift is involved (i.e., reaction time or
181 premature triggering of the timing equipment). Comparing the split times of Mike and
182 John in Figure 1, it can be noticed that the lines are parallel. In this scenario, the
183 *Estimated TC* model can remove bias between Mike and John. The *Estimated TC* model
184 can also help remove bias in estimated parameters in Phil's case. However, when
185 looking closely at Figure 1, it can be noticed that Phil's and Mike's lines are not
186 parallel. This is because there is already some velocity when the initial timing gate is
187 triggered; thus, the time shift is not constant.

188 These models (i.e., *Fixed TC* of +0.3, +0.5 s, and *Estimated TC* model) are applied to
 189 Mike, Phil, and John's split times. The estimated model parameters can be found in
 190 Table 3, and previously estimated parameter values using the *No correction* model. As
 191 can be noted from Table 3, adding +0.3 s worked well for Phil in terms of approaching
 192 *true* parameter values, while adding +0.5 s was detrimental in un-biasing estimated
 193 parameters. The *Estimated TC* model worked well for all three athletes in terms of un-
 194 biasing the parameter estimates. The estimated TC parameter for John was also very
 195 close to the *true* reaction time of 0.2 s.

196 *Estimated flying distance model*

197 Although the *Estimated TC* model performed well in Phil's case (triplet brother doing
 198 flying start), instead of assuming time shift (which helps in un-biasing the estimates
 199 compared to the *No correction* model), the model definition that assumes *flying start*
 200 *distance* (FD) involved in the *data-generating-process* (DGP) can be utilized. This
 201 *Estimated FD* model utilizes Equation 8 as the model definition.

$$202 \quad t(d) = \left(TAU \times W \left(-e^{\frac{-d+FD}{MSS \times TAU}} - 1 \right) + \frac{d + FD}{MSS} + TAU \right) - \left(TAU \times W \left(-e^{\frac{FD}{MSS \times TAU}} - 1 \right) + \frac{FD}{MSS} + TAU \right) \quad (8)$$

203 Table 3 contains all model estimates for three brothers, including the *Estimated FD*
 204 model. It can be noticed that the *Estimated FD* model unbiased estimates for Phil but
 205 failed to be estimated for John (brother that starts at gunfire and has reaction time
 206 involved in his split times). This is because the *Estimated FD* model is *ill-defined* under
 207 that scenario and cannot have a *negative* flying distance.

208 Overall, each model definition has assumed the mechanism of the data generation. *No*
 209 *correction* model assumes perfect synchronization of the sprint initiation with the start
 210 of the timing. The *Estimated TC* model introduces a simple intercept that can help

211 estimate parameters when an assumed time shift is involved (e.g., when reaction time is
212 involved or premature triggering of the initial timing gate). *Estimated TC* can also be
213 used when flying start is utilized, but it assumes the constant time shift, which is not the
214 case in that scenario due to already gained velocity at the start. The *Estimated FD*
215 model assumes there is a flying sprint involved in the DGP and, as shown in Table 3,
216 can be ill-defined when there is no flying distance involved but there is a time shift. All
217 three models assume athlete accelerates according to the mono-exponential Equation 1.

218

219 **[Insert Table 3 here]**

220

221 ***Simulation design***

222 To explore the behavior of these three models under simulated and known conditions,
223 short sprints data is generated using *true* MSS (ranging from 7 to 11 ms^{-1} , in
224 increments of 0.05 ms^{-1} , resulting in a total of 81 unique values), MAC (ranging from
225 7 to 11 ms^{-2} , in increments of 0.05 ms^{-2} , resulting in a total of 81 unique values), and
226 flying distance (ranging from 0 to 0.5 m , in increments of 0.01 m , resulting in a total of
227 51 unique values). Each flying sprint distance consisted of 6,561 MSS and MAC
228 combinations. Split times are estimated using timing gates positioned at 5, 10, 20, 30,
229 and 40 m , with the rounding to the closest 10 ms . In total, there were 334,611 sprints
230 simulated.

231 ***Statistical analysis***

232 MSS, MAC, TAU, and PMAX are estimated for each simulated sprint using the *No*
233 *correction*, *Estimated TC*, and *Estimated FD models*. The agreement between *true* and

234 estimated parameter values is evaluated using the *percent difference* (*%Diff*) estimator
235 (Equation 9).

$$236 \quad \%Diff = 100 \times \frac{estimated - true}{true} \quad (9)$$

237 The distribution of the simulated *%Diff* is summarized using *median* and 95%
238 *highest-density continuous interval* (*HDCI*) (Kruschke 2015; Kruschke and Liddell
239 2018a; Kruschke and Liddell 2018b; Kruschke 2018; Makowski et al. 2019). To
240 provide magnitude interpretation of the *%Diff*, *region of practical equivalence*
241 (*ROPE*), as well as the proportion of the simulations that lie within *ROPE*
242 (*inside ROPE*; expressed as a percentage) (Kruschke 2015; Kruschke and Liddell
243 2018a; Kruschke and Liddell 2018b; Kruschke 2018; Makowski et al. 2019; Jovanović
244 2020), are calculated. *ROPE* is assumed to be equal to 95% *HDCI* of the *%Diff* using
245 the *No correction* model and no flying distance. Theoretically, *ROPE* represents the
246 lowest error (i.e., the best agreement) that can be achieved. It is limited purely by the
247 timing gates' measurement precision (i.e., rounding to the closest 10 *ms*) and simulated
248 parameters.

249 In addition to estimating agreement between *true* and estimated parameter values,
250 practitioners are often interested in whether they can use estimated values to track
251 changes in the *true* parameter values. A *minimal detectable change* estimator with 95%
252 confidence (*%MDC₉₅*) (Furlan and Sterr 2018; Jovanović 2020) is utilized to estimate
253 this sensitivity. The *%MDC₉₅* value might be regarded as the minimum amount of
254 change that needs to be observed in the estimated parameter for it to be considered a
255 *true* change. *%MDC₉₅* is calculated using *percent residual standard error* (*%RSE*;
256 Equation 10) of the linear regression between *true* (predictor) and estimated parameter
257 values (outcome) (Equation 11). Since simulated data with the known *true* values are

258 utilized, %RSE represents the *percent standard error of the measurement* (%SEM) in
259 the estimated parameters.

$$260 \quad \%RSE = \sqrt{\frac{\sum_{i=1}^N \left(100 \times \frac{y_i - \hat{y}_i}{\hat{y}_i}\right)^2}{N - 2}} \quad (10)$$

$$261 \quad \%MDC_{95} = \%RSE \times \sqrt{2} \times 1.96 \quad (11)$$

262 In addition to providing %MDC₉₅ for the estimated parameters, the lowest %MDC₉₅ is
263 estimated using the *No correction* model and no flying distance (%MDC₉₅^{lowest}).

264 Theoretically, %MDC₉₅^{lowest} represents the lowest %MDC₉₅ that can be achieved, and it
265 is limited purely by the timing gates' measurement precision (i.e., rounding to the
266 closest 10 ms) and simulated parameters. %MDC₉₅^{lowest} is used only as a reference to
267 evaluate estimated parameters' %MDC₉₅.

268 The analyses are performed on both *pooled* dataset (i.e., using all flying distances) and
269 across every flying distance. It is hypothesized that the *Estimated FD* model will have
270 the highest *inside ROPE* estimates and the lowest %MDC₉₅ estimates. Statistical
271 analyses and graph construction were performed using the software R 4.2.1 (R Core
272 Team 2022) in RStudio (version 2022.07.1+554).

273 **Results**

274 ***Model fitting***

275 Table 4 contains failed model fitting for the *Estimated FD* model. These were
276 disregarded from further analysis. The reason for these failed model fittings is probably
277 the combination of the very small flying distance and the measurement precision of the
278 timing gates, resulting in an ill-defined model that cannot be fitted.

279

280 **[Insert Table 4 here]**

281 *Percent difference*

282 *Region of practical equivalence*

283 Estimated ROPEs are equal to -0.3 to 0.33% for MSS, -0.73 to 0.74% for MAC, -1.03
284 to 1% for TAU, and -0.5 to 0.5% for PMAX (Table 5) and are depicted as grey
285 horizontal bars in Figure 2 and Figure 3.

286 *Pooled analysis*

287 The pooled analysis is performed using all flying distances pooled together. As such,
288 the pooled analysis represents the overall estimate of the agreement between *true* and
289 estimated parameter values across simulated conditions. Figure 2 depicts the
290 distribution of the pooled *%Diff* estimator. Table 5 contains the pooled analysis results
291 summary for every model and short sprint parameter.

292

293 **[Insert Figure 2 here]**

294 **[Insert Table 5 here]**

295 *Analysis across flying distances*

296 Figure 3 depicts the analysis results for every flying distance in the simulation.

297 *Inside ROPE* parameter estimates are calculated and depicted in Figure 4 for easier
298 comprehension.

299 **[Insert Figure 3 here]**

300 **[Insert Figure 4 here]**

301 ***Minimal detectable change***

302 *Lowest Minimum Detectable Change*

303 Estimated $\%MDCs_{95}^{lowest}$ is equal to 0.45% for MSS, 1.06% for MAC, 1.47% for TAU,
304 and 0.7% for PMAX (column *lowest* in Table 6) and dashed grey horizontal lines in
305 Figure 5.

306 *Pooled analysis*

307 Estimated parameters' $\%MDCs_{95}$ for the *No correction* model range from 3 to 44%, for
308 the *Estimated TC* range from 1 to 8%, and for the *Estimated FD* range from 1 to 7%
309 (Table 6).

310

311 **[Insert Table 6 here]**

312 *Analysis across flying distances*

313 The estimated $\%MDCs_{95}$ across flying distances are depicted in Figure 5. For every
314 short sprint parameter, *Estimated TC* showed stable and lower $\%MDCs_{95}$ compared to
315 *Estimated FD* (from 1 to 6% and from 1 to 8%, respectively). The *No correction* model
316 showed the lowest $\%MDCs_{95}$ for the MAC and TAU parameters, ranging from 1 to 5%
317 and from 1 to 3%, respectively.

318

319 **[Insert Figure 5 here]**

320 **Discussion**

321 The aim of this study was to estimate the agreement between *true* short sprint
322 parameter values and *estimated* parameter values using three model definitions
323 under simulated conditions. This agreement is estimated using the %*Diff*
324 estimator (Equation 9). In addition to estimating agreement, this study aims to
325 estimate the sensitivity of the models to detect changes in *true* short sprint
326 parameter values. This sensitivity is estimated using the %*MDC*₉₅ estimator
327 (Equation 11). Agreement and sensitivity analysis is performed using the *pooled*
328 dataset and across simulated flying sprint distances.

329

330 *Agreement between true and estimated short sprint parameters*

331 *Region of practical equivalence*

332 An interesting finding is that, given simulation parameters (particularly the precision of
333 the timing gates to the closest 10 *ms*), MSS has the lowest *ROPE* compared to other
334 short sprint parameters (Table 5 and Figure 2). Since *ROPE* represents the lowest
335 estimation error, MSS is the parameter that could be, given this theoretical simulation,
336 estimated with the most precision. In contrast, TAU and MAC can be estimated with the
337 least precision.

338 *Pooled analysis*

339 As expected, the *Estimated FD* model performed with the highest *inside ROPE*
340 parameter values (from 20 to 72%), with the narrowest 95% *HDCIs* (from -5 to 5%),
341 and no bias involved (Table 5 and Figure 2). On the other hand, the *No correction*
342 model performed poorly, with the lowest *inside ROPE* parameter values (from 2 to 2%),

343 with the widest 95% *HDCIs* (from -46 to 80%), and with the apparent bias indicated
344 with the *median* parameter values being outside of *ROPE* (from -35 to 49%) (Table 5
345 and Figure 2). In addition, a visual inspection of Figure 2 indicates a *non-normal*
346 distribution of estimated %*Diff* parameter values, demanding further analysis across
347 flying distance values. The *Estimated TC* model performed similarly to the *Estimated*
348 *FD* model with a slightly lower *inside ROPE* parameter values (from 9 to 67%), wider
349 95% *HDCIs* (from -9 to 8%), and with obvious bias, although much smaller than the *No*
350 *correction* model bias (from -3 to 3%) (Table 5 and Figure 2).

351 *Analysis across flying distances*

352 As expected, the *No correction* model demonstrated increasing bias as the flying
353 distance increased (from -46 to 76%), the widest 95% *HDCIs* (from -47 to 84%), and
354 the lowest *inside ROPE* estimated parameter values (Figures 3 and 4). *Estimated TC*
355 showed a small bias trend across flying distances (from -6 to 6%), resulting in
356 decreasing *inside ROPE* performance (from 0 to 75%; see Figure 4), although with
357 much smaller 95% *HDCIs* (from -10 to 11%) compared to *No correction* model.
358 *Estimated FD*, as hypothesized, showed no bias and thus a stable *inside ROPE*
359 performance across flying distances (see Figure 4), with minimal 95% *HDCIs* (from -5
360 to 6%).

361 *Sensitivity to detect changes in true short sprint parameters*

362 *Lowest Minimum Detectable Change*

363 An interesting finding is that, given simulation parameters (particularly the precision of
364 the timing gates to the closest 10 *ms*), MSS has the lowest % MDC_{95}^{lowest} compared to
365 other short sprint parameters (Table 6). Since % MDC_{95}^{lowest} represents the lowest

366 minimal detectable change, MSS is the parameter whose change could be, given this
367 theoretical simulation, estimated with the most precision. In contrast, TAU and MAC
368 changes can be estimated with the least precision.

369 *Pooled analysis*

370 Pooled % $MDC_{S_{95}}$ represents an estimate of the *sensitivity* to detect *true* change with
371 95% confidence when the flying start distance is not standardized (but within simulation
372 parameter limits (ranging from 0 to 0.5 m). As expected, the *No correction* model
373 demonstrates the highest % $MDC_{S_{95}}$ (from 3 to 44%), while *Estimated TC* and
374 *Estimated FD* demonstrated much smaller % $MDC_{S_{95}}$ (from 1 to 8% and from 1 to 7%,
375 respectively) (Table 6).

376 An interesting finding is that the MSS parameter showed very low % $MDC_{S_{95}}$ across
377 models (from 1 to 3%), even for the *No correction* model. This indicates that even the
378 non-standardized short sprint monitoring (i.e., without standardized flying distance)
379 using the *No correction* model, given simulation parameters, can be used to track
380 changes in MSS. TAU, MAC, and PMAX parameters, on the other hand, demand a
381 much larger % $MDC_{S_{95}}$ (from 7 to 44%, from 6 to 37%, and from 6 to 36%,
382 respectively).

383 *Analysis across flying distances*

384 When estimated across flying distances, % $MDC_{S_{95}}$ shows interesting and surprising
385 patterns (Figure 5). For every short sprint parameter, *Estimated TC* showed stable and
386 lower % $MDC_{S_{95}}$ compared to *Estimated FD* (from 1 to 6% and from 1 to 8%,
387 respectively). This is surprising because even if it demonstrated biased estimates of
388 short sprint parameters (Figures 3 and 4) compared to the *Estimated FD*, *Estimated TC*
389 might be more sensitive to detect *changes*, given simulation parameters.

390 Another surprising finding is that the *No correction* model, even if shown to be highly
391 biased in estimating short sprint parameter values (Figures 3 and 4), showed the lowest
392 $\%MDC_{S_{95}}$ for the MAC and TAU parameters (from 1 to 5% and from 1 to 3%
393 respectively). This indicates that when short sprint measurement is standardized (i.e.,
394 athletes perform with the same flying distance), given the simulation parameters, the *No*
395 *correction* model can be the most sensitive model to detect *changes* in MAC and TAU
396 parameters. This is unfortunately not the case for the MSS and PMAX parameters (from
397 0 to 3% and from 1 to 9%, respectively) (Figure 5).

398 Overall, when it comes to estimating *changes* in short sprint parameters, *change* in MSS
399 is the most sensitive to be detected (from 0 to 3%) compared to MAC (from 1 to 7%),
400 TAU (from 1 to 8%), and PMAX (from 1 to 9%) (Figure 5).

401 ***Conclusions***

402 The simulation study employed demonstrated some expected and unexpected theoretical
403 findings. Among the expected findings are (1) the bias and low *inside ROPE*
404 performance in estimating short sprint parameters using the *No correction* model, (2)
405 more negligible bias and higher *inside ROPE* for the *Estimated TC* model, and (3) no
406 bias and highest *inside ROPE* for the *Estimated FD* model. The unexpected finding of
407 this study is the performance of the *No correction* model in sensitivity of estimating the
408 *change* of the MAC and TAU parameters, which outperformed the other two models.

409 When estimating short sprint parameters across models, given simulation parameters,
410 MSS and *change* in MSS can be estimated more precisely compared to TAU, MAC,
411 and PMAX parameters and their *changes*.

412 In addition to model performances, this simulation study provided the theoretical
413 *ROPEs* and $\%MDC_{S_{95}}^{lowest}$ estimates. These could be useful for further validity and

414 reliability studies evaluating short sprint model performance involving *real* athletes by
415 providing minimal theoretical values one can achieve with timing gates positioned at
416 the exact distances with the exact time rounding.

417 The takeaway message for the practitioners is that besides standardizing the sprint
418 starting technique for the short sprint performance monitoring, it would be wise to
419 utilize and track the results of all three models. The *Estimated FD* model will provide
420 unbiased estimates of the current performance, but the *No correction* model might be
421 more sensitive in detecting changes in TAU and MAC parameters.

422 This practical conclusion should be taken with caution since it is based on the results of
423 this theoretical simulation. Additional studies involving *real* athletes in evaluating the
424 performance of these three models are needed. These studies should involve estimating
425 the short sprint parameters agreement between gold-standard (i.e., *criterion*) measure
426 (e.g., radar gun, laser gun, or video analysis) and *practical* measure using timing gates
427 with different timing initiation (e.g., crossing the beam, foot pressing on force sensor or
428 leaving the ground) under different flying start conditions and distances (e.g., start on
429 the line, start at 0.5 m behind the initial timing gate, use of body-rocking) to practically
430 demonstrate bias introduced when timing initiation is not synchronizes with initial force
431 application. In addition to theoretical findings, such studies will provide model
432 performance estimates when biological variability is involved in short sprints, which is
433 not considered in the current study. One such study is currently in preparation.

434 **Data availability statement**

435 The data that support the findings of this study are openly available in the GitHub
436 repository at <https://github.com/mladenjovanovic/shorts-simulation-paper> (DOI:
437 10.5281/zenodo.7094284), as well as the reproducible *Quarto* (Allaire et al. 2022)
438 source code.

439 **Declaration of interest statement**

440 The author report there are no competing interests to declare

441 **References**

442 Allaire JJ, Teague C, Scheidegger C, Xie Y, Dervieux C. 2022. Quarto [Internet]. [place
443 unknown]. <https://doi.org/10.5281/zenodo.5960048>

444

445 Altmann S, Hoffmann M, Kurz G, Neumann R, Woll A, Haertel S. 2015. Different
446 Starting Distances Affect 5-m Sprint Times. *Journal of Strength and Conditioning*
447 *Research* [Internet]. [accessed 2021 Jun 21] 29(8):2361–2366.

448 <https://doi.org/10.1519/JSC.0000000000000865>

449

450 Altmann S, Spielmann M, Engel FA, Neumann R, Ringhof S, Oriwol D, Haertel S.
451 2017. Validity of Single-Beam Timing Lights at Different Heights. *Journal of Strength*
452 *and Conditioning Research* [Internet]. [accessed 2021 Jun 21] 31(7):1994–1999.

453 <https://doi.org/10.1519/JSC.0000000000001889>

454

455 Altmann S, Spielmann M, Engel FA, Ringhof S, Oriwol D, Härtel S, Neumann R. 2018.
456 Accuracy of single beam timing lights for determining velocities in a flying 20-m sprint:
457 Does timing light height matter? *jhse* [Internet]. [accessed 2021 Jun 21] 13(3).

458 <https://doi.org/10.14198/jhse.2018.133.10>

459

460 Brown TD, Vescovi JD, Vanheest JL. 2004. Assessment of linear sprinting
461 performance: A theoretical paradigm. *Journal of Sports Science & Medicine*. 3(4):203–
462 210.

463

464 Buchheit M, Samozino P, Glynn JA, Michael BS, Al Haddad H, Mendez-Villanueva A,
465 Morin JB. 2014. Mechanical determinants of acceleration and maximal sprinting speed
466 in highly trained young soccer players. *Journal of Sports Sciences*. 32(20):1906–1913.
467 <https://doi.org/10.1080/02640414.2014.965191>
468

469 Clark KP, Rieger RH, Bruno RF, Stearne DJ. 2017. The NFL Combine 40-Yard Dash:
470 How Important is Maximum Velocity? *Journal of Strength and Conditioning*
471 *Research*.:1. <https://doi.org/10.1519/JSC.0000000000002081>
472

473 Corless RM, Gonnet GH, Hare DEG, Jeffrey DJ, Knuth DE. 1996. On the LambertW
474 function. *Adv Comput Math* 5(1):329–359. <https://doi.org/10.1007/BF02124750>
475

476 Edwards T, Piggott B, Banyard HG, Haff GG, Joyce C. 2020. Sprint acceleration
477 characteristics across the Australian football participation pathway. *Sports*
478 *Biomechanics*.:1–13. <https://doi.org/10.1080/14763141.2020.1790641>
479

480 Elzhov TV, Mullen KM, Spiess A-N, Bolker B. 2022. Minpack.lm: R interface to the
481 levenberg-marquardt nonlinear least-squares algorithm found in MINPACK, plus
482 support for bounds [Internet]. [place unknown]. [https://CRAN.R-](https://CRAN.R-project.org/package=minpack.lm)
483 [project.org/package=minpack.lm](https://CRAN.R-project.org/package=minpack.lm)
484

485 Furlan L, Sterr A. 2018. The Applicability of Standard Error of Measurement and
486 Minimal Detectable Change to Motor Learning Research—A Behavioral Study. *Front*
487 *Hum Neurosci* [Internet]. [accessed 2022 Jul 15] 12:95.
488 <https://doi.org/10.3389/fnhum.2018.00095>

489

490 Furusawa K, Hill AV, Parkinson JL. 1927. The dynamics of "sprint" running.

491 Proceedings of the Royal Society of London Series B, Containing Papers of a

492 Biological Character. 102(713):29–42. <https://doi.org/10.1098/rspb.1927.0035>

493

494 Goerg GM. 2022. LambertW: Probabilistic models to analyze and gaussianize heavy-

495 tailed, skewed data [Internet]. [place unknown]. [https://CRAN.R-](https://CRAN.R-project.org/package=LambertW)

496 [project.org/package=LambertW](https://CRAN.R-project.org/package=LambertW)

497

498 Haugen TA, Breitschädel F, Samozino P. 2020. Power-Force-Velocity Profiling of

499 Sprinting Athletes: Methodological and Practical Considerations When Using Timing

500 Gates. *Journal of Strength and Conditioning Research*. 34(6):1769–1773.

501 <https://doi.org/10.1519/JSC.0000000000002890>

502

503 Haugen TA, Breitschädel F, Seiler S. 2019. Sprint mechanical variables in elite athletes:

504 Are force-velocity profiles sport specific or individual? Peyré-Tartaruga LA, editor.

505 *PLOS ONE*. 14(7):e0215551. <https://doi.org/10.1371/journal.pone.0215551>

506

507 Haugen TA, Breitschädel F, Seiler S. 2020. Sprint mechanical properties in soccer

508 players according to playing standard, position, age and sex. *Journal of Sports Sciences*.

509 38(9):1070–1076. <https://doi.org/10.1080/02640414.2020.1741955>

510

511 Haugen TA, Tønnessen E, Seiler SK. 2012. The Difference Is in the Start: Impact of

512 Timing and Start Procedure on Sprint Running Performance: *Journal of Strength and*

513 *Conditioning Research*. 26(2):473–479. <https://doi.org/10.1519/JSC.0b013e318226030b>

514

515 Haugen T, Buchheit M. 2016. Sprint Running Performance Monitoring: Methodological
516 and Practical Considerations. *Sports Med* [Internet]. [accessed 2021 Jul 16] 46(5):641–
517 656. <https://doi.org/10.1007/s40279-015-0446-0>

518

519 Jiménez-Reyes P, Samozino P, García-Ramos A, Cuadrado-Peñafiel V, Brughelli M,
520 Morin J-B. 2018. Relationship between vertical and horizontal force-velocity-power
521 profiles in various sports and levels of practice. *PeerJ*. 6:e5937.
522 <https://doi.org/10.7717/peerj.5937>

523

524 Jovanović M. 2020. *Bmbstats: Bootstrap Magnitude-based Statistics for Sports*
525 *Scientists*. Belgrade, Serbia. Mladen Jovanović, ISBN: 978-8690080359.

526

527 Jovanović M. 2022. *Shorts: Short sprints* [Internet]. [place unknown]. [https://CRAN.R-](https://CRAN.R-project.org/package=shorts)
528 [project.org/package=shorts](https://CRAN.R-project.org/package=shorts)

529

530 Jovanović M, Vescovi J. 2022. *Shorts: An R package for modeling short sprints*.

531 *International Journal of Strength and Conditioning* [Internet]. 2(1).

532 <https://doi.org/10.47206/ijsc.v2i1.74>

533

534 Kruschke JK. 2015. *Doing Bayesian data analysis: A tutorial with R, JAGS, and Stan*.

535 Edition 2. Boston: Academic Press.

536

537 Kruschke JK. 2018. Rejecting or Accepting Parameter Values in Bayesian Estimation.
538 Advances in Methods and Practices in Psychological Science [Internet]. [accessed 2022
539 Jul 10] 1(2):270–280. <https://doi.org/10.1177/2515245918771304>
540

541 Kruschke JK, Liddell TM. 2018a. Bayesian data analysis for newcomers. Psychonomic
542 Bulletin & Review [Internet]. [accessed 2019 Sep 17] 25(1):155–177.
543 <https://doi.org/10.3758/s13423-017-1272-1>
544

545 Kruschke JK, Liddell TM. 2018b. The Bayesian New Statistics: Hypothesis testing,
546 estimation, meta-analysis, and power analysis from a Bayesian perspective.
547 Psychonomic Bulletin & Review [Internet]. [accessed 2019 Sep 17] 25(1):178–206.
548 <https://doi.org/10.3758/s13423-016-1221-4>
549

550 Makowski D, Ben-Shachar M, Lüdtke D. 2019. bayestestR: Describing Effects and
551 their Uncertainty, Existence and Significance within the Bayesian Framework. Journal
552 of Open Source Software [Internet]. [accessed 2019 Sep 23] 4(40):1541.
553 <https://doi.org/10.21105/joss.01541>
554

555 Mangine GT, Hoffman JR, Gonzalez AM, Wells AJ, Townsend JR, Jajtner AR,
556 McCormack WP, Robinson EH, Fragala MS, Fukuda DH, Stout JR. 2014. Speed,
557 Force, and Power Values Produced From Nonmotorized Treadmill Test Are Related to
558 Sprinting Performance: Journal of Strength and Conditioning Research. 28(7):1812–
559 1819. <https://doi.org/10.1519/JSC.0000000000000316>
560

561 Marcote-Pequeño R, García-Ramos A, Cuadrado-Peñañiel V, González-Hernández JM,
562 Gómez MÁ, Jiménez-Reyes P. 2019. Association Between the Force and Performance
563 Variables Obtained in Jumping and Sprinting in Elite Female Soccer Players.
564 International Journal of Sports Physiology and Performance. 14(2):209–215.
565 <https://doi.org/10.1123/ijsp.2018-0233>
566
567 Morin JB. 2017. A spreadsheet for Sprint acceleration Force-Velocity-Power profiling
568 [Internet]. [accessed 2020 Oct 27]. [https://jbmorin.net/2017/12/13/a-spreadsheet-for-](https://jbmorin.net/2017/12/13/a-spreadsheet-for-sprint-acceleration-force-velocity-power-profiling/)
569 [sprint-acceleration-force-velocity-power-profiling/](https://jbmorin.net/2017/12/13/a-spreadsheet-for-sprint-acceleration-force-velocity-power-profiling/)
570
571 Morin J-B, Samozino P, Murata M, Cross MR, Nagahara R. 2019. A simple method for
572 computing sprint acceleration kinetics from running velocity data: Replication study
573 with improved design. Journal of Biomechanics. 94:82–87.
574 <https://doi.org/10.1016/j.jbiomech.2019.07.020>
575
576 Motulsky H. 2018. Intuitive biostatistics: A nonmathematical guide to statistical
577 thinking. Fourth edition. New York: Oxford University Press.
578
579 R Core Team. 2022. R: A language and environment for statistical computing [Internet].
580 Vienna, Austria: R Foundation for Statistical Computing. <https://www.R-project.org/>
581
582 Samozino P, Rabita G, Dorel S, Slawinski J, Peyrot N, Saez de Villarreal E, Morin J-B.
583 2016. A simple method for measuring power, force, velocity properties, and mechanical
584 effectiveness in sprint running: Simple method to compute sprint mechanics.

585 Scandinavian Journal of Medicine & Science in Sports. 26(6):648–658.
586 <https://doi.org/10.1111/sms.12490>
587
588 Stenroth L, Vartiainen P. 2020. Spreadsheet for sprint acceleration force-velocity-power
589 profiling with optimization to correct start time.
590 <https://doi.org/10.13140/RG.2.2.12841.83045>
591
592 Stenroth L, Vartiainen P, Karjalainen PA. 2020. Force-velocity profiling in ice hockey
593 skating: Reliability and validity of a simple, low-cost field method. Sports
594 Biomechanics.:1–16. <https://doi.org/10.1080/14763141.2020.1770321>
595
596 Vescovi JD, Jovanović M. 2021. Sprint Mechanical Characteristics of Female Soccer
597 Players: A Retrospective Pilot Study to Examine a Novel Approach for Correction of
598 Timing Gate Starts. Front Sports Act Living [Internet]. [accessed 2021 Jul 1] 3:629694.
599 <https://doi.org/10.3389/fspor.2021.629694>
600
601 Ward-Smith AJ. 2001. Energy conversion strategies during 100 m sprinting. Journal of
602 Sports Sciences. 19(9):701–710. <https://doi.org/10.1080/02640410152475838>
603

604 **Table 1:** Sample split times measured during 40 *m* sprint performance using timing
605 gates positioned at 5, 10, 20, 30, and 40 *m*.

Distance (m)	Split time (s)
5	1.34
10	2.06
20	3.29
30	4.44
40	5.56

606

607

608 **Table 2:** Estimated sprint parameters for Mike, Phil, and John. All three brothers have
 609 identical sprint performance but utilize different sprint starts, which results in different
 610 split times, and thus different sprint parameter estimates. Due to the timing gates'
 611 precision to 2 decimals (i.e., 10 *ms*), estimated Mike's parameters also differ from the
 612 *true* values.

Athlete	MSS	TAU	MAC	PMAX
<i>True</i>	9.00	1.12	8.00	18.0
Mike (theoretical)	9.02	1.14	7.94	17.9
Phil (flying start)	8.60	0.61	14.00	30.1
John (gunfire)	9.59	1.62	5.93	14.2

613 *Note.* MSS – maximum sprinting speed (expressed in ms^{-1}); TAU – relative acceleration (expressed in seconds); MAC – maximum
 614 acceleration (expressed in ms^{-2}); PMAX – maximal relative power (expressed in W/kg)

615

616 **Table 3:** Estimated sprint parameters for Mike, Phil, and John for (1) *No correction*, (2)
617 *Fixed time corrections* (Fixed TC) with +0.3s and +0.5s corrections, (3) *Estimated time*
618 *correction* (Estimated TC), and (4) *Estimated flying start distance* (Estimated FD)
619 models.

Model	Athlete	MSS	TAU	MAC	PMAX	TC	FD
	<i>True</i>	<i>9.00</i>	<i>1.12</i>	<i>8.00</i>	<i>18.0</i>		
No correction	Mike (theoretical)	9.02	1.14	7.94	17.9		
	Phil (flying start)	8.60	0.61	14.00	30.1		
	John (gunfire)	9.59	1.62	5.93	14.2		
Fixed +0.3s TC	Mike (theoretical)	10.01	1.93	5.19	13.0		
	Phil (flying start)	9.05	1.13	8.02	18.2		
	John (gunfire)	11.29	2.79	4.05	11.4		
Fixed +0.5s TC	Mike (theoretical)	11.29	2.79	4.05	11.4		
	Phil (flying start)	9.62	1.61	5.98	14.4		
	John (gunfire)	13.67	4.26	3.21	11.0		
Estimated TC	Mike (theoretical)	9.04	1.15	7.86	17.8	0.01	
	Phil (flying start)	9.00	1.08	8.35	18.8	0.28	
	John (gunfire)	9.04	1.15	7.86	17.8	-0.19	
Estimated FD	Mike (theoretical)	9.04	1.15	7.86	17.8		0.00
	Phil (flying start)	9.03	1.16	7.82	17.7		0.54
	John (gunfire) ^a						

620 *Note.* MSS – maximum sprinting speed (expressed in ms^{-1}); TAU – relative acceleration (expressed in seconds); MAC – maximum
621 acceleration (expressed in ms^{-2}); PMAX – maximal relative power (expressed in W/kg); TC – time correction (expressed in
622 second); FD – flying start distance (expressed in meters)

623 ^a Failed to be estimated due to the ill-defined model for the time-reaction scenario

624 **Table 4:** Failed model fittings for the *Estimated flying start distance* (Estimated FD)
625 model.

Flying distance (m)	Not fitted	Total	Not fitted (%)
0.00	1765	6561	26.90
0.01	12	6561	0.18
0.02	16	6561	0.24
0.03	10	6561	0.15
0.04	4	6561	0.06
0.05	1	6561	0.02

626

627 **Table 5:** Region of practical equivalence (*ROPE*), a summary of percent difference
628 (*%Diff*) distribution, and percentage of the simulations that lie within the region of
629 practical equivalence (*inside ROPE*) estimated using pooled simulation dataset for (1)
630 *No correction*, (2) *Estimated time correction* (Estimated TC), and (3) *Estimated flying*
631 *start distance* (Estimated FD) models.

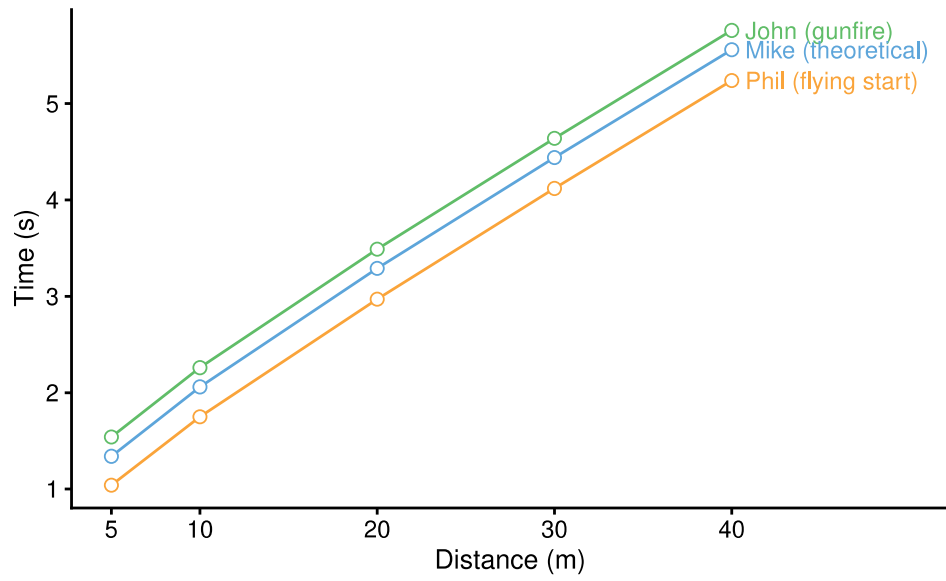
Parameter	ROPE (%)	Model	% Diff	Inside ROPE (%)
MSS	-0.3 to 0.33%	No correction	median -3%, 95% HDCI [-7 to 0%]	2%
		Estimated TC	median 0%, 95% HDCI [-1 to 0%]	67%
		Estimated FD	median 0%, 95% HDCI [-1 to 1%]	72%
MAC	-0.73 to 0.74%	No correction	median 49%, 95% HDCI [11 to 80%]	2%
		Estimated TC	median 3%, 95% HDCI [-2 to 8%]	12%
		Estimated FD	median 0%, 95% HDCI [-4 to 4%]	25%
TAU	-1.03 to 1%	No correction	median -35%, 95% HDCI [-46 to -11%]	2%
		Estimated TC	median -3%, 95% HDCI [-9 to 2%]	16%
		Estimated FD	median 0%, 95% HDCI [-5 to 5%]	31%
PMAX	-0.5 to 0.5%	No correction	median 44%, 95% HDCI [6 to 73%]	2%
		Estimated TC	median 3%, 95% HDCI [-2 to 8%]	9%
		Estimated FD	median 0%, 95% HDCI [-4 to 4%]	20%

632 *Note.* MSS – maximum sprinting speed; TAU – relative acceleration; MAC – maximum acceleration; PMAX – maximal relative
633 power HDCI - highest-density continuous interval

634 **Table 6:** Minimal detectable change using 95% confidence level ($\%MDC_{S_{95}}$)
 635 estimated using pooled simulation dataset for (1) *No correction*, (2) *Estimated time*
 636 *correction* (Estimated TC), and (3) *Estimated flying start distance* (Estimated FD)
 637 models.

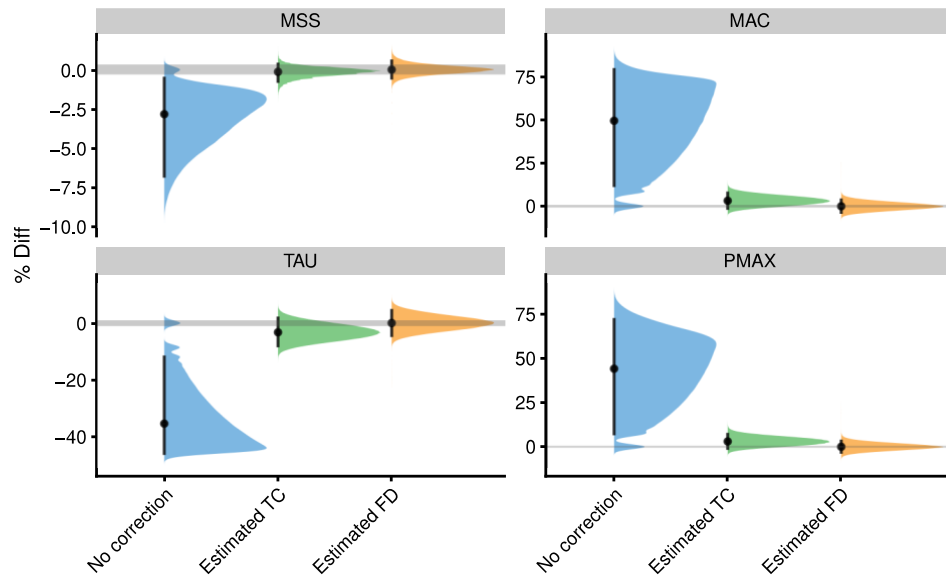
Parameter	lowest	No correction	Estimated TC	Estimated FD
MSS	0.45 %	3 %	1 %	1 %
MAC	1.06 %	37 %	7 %	6 %
TAU	1.47 %	44 %	8 %	7 %
PMAX	0.7 %	36 %	7 %	6 %

638 *Note.* MSS – maximum sprinting speed; TAU – relative acceleration; MAC – maximum acceleration; PMAX – maximal relative
 639 power



640

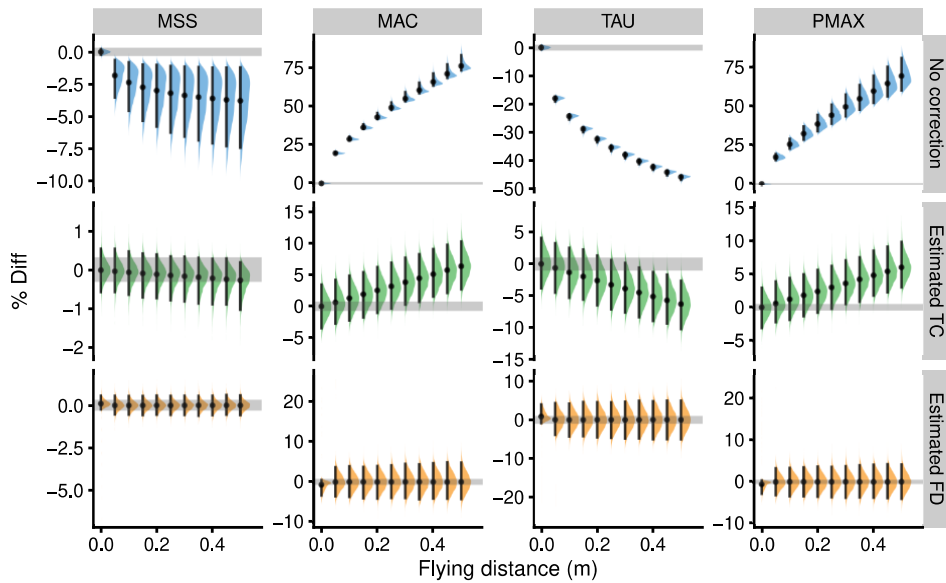
641 **Figure 1:** Phil, Mike, and John split times over a 40 m distance. All three brothers have
642 identical sprint performances but utilize different sprint starts, resulting in different split
643 times.



644

645 **Figure 2:** Pooled distribution of the percent difference ($\%Diff$) for (1) *No correction*,
 646 (2) *Estimated time correction* (Estimated TC), and (3) *Estimated flying start distance*
 647 (Estimated FD) models. Error bars represent the distribution *median* and 95% highest-
 648 density continuous interval (95% *HDCI*). A grey area represents the parameter region
 649 of practical equivalence (*ROPE*) (assumed to be equal to 95% *HDCI* of the $\%Diff$
 650 using the *No correction* model and no flying distance).

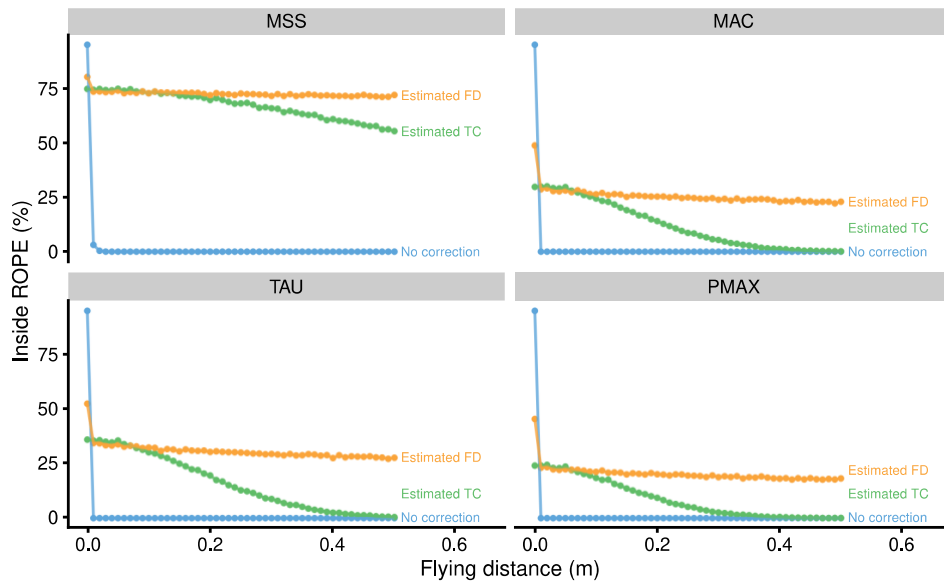
651 *Note.* MSS – maximum sprinting speed; TAU – relative acceleration; MAC – maximum acceleration; PMAX – maximal relative
 652 power



653

654 **Figure 3:** Distribution of the percent difference ($\%Diff$) across every flying distance in
 655 the simulation for (1) *No correction*, (2) *Estimated time correction* (Estimated TC), and
 656 (3) *Estimated flying start distance* (Estimated FD) models. Error bars represent the
 657 distribution *median* and 95% highest-density continuous interval (95% *HDCI*). A grey
 658 area represents the parameter region of practical equivalence (*ROPE*) (assumed to be
 659 equal to 95% *HDCI* of the $\%Diff$ using the *No correction* model and no flying
 660 distance). For the less crowded visualization, flying distance in increments of 0.05 *m* is
 661 plotted.

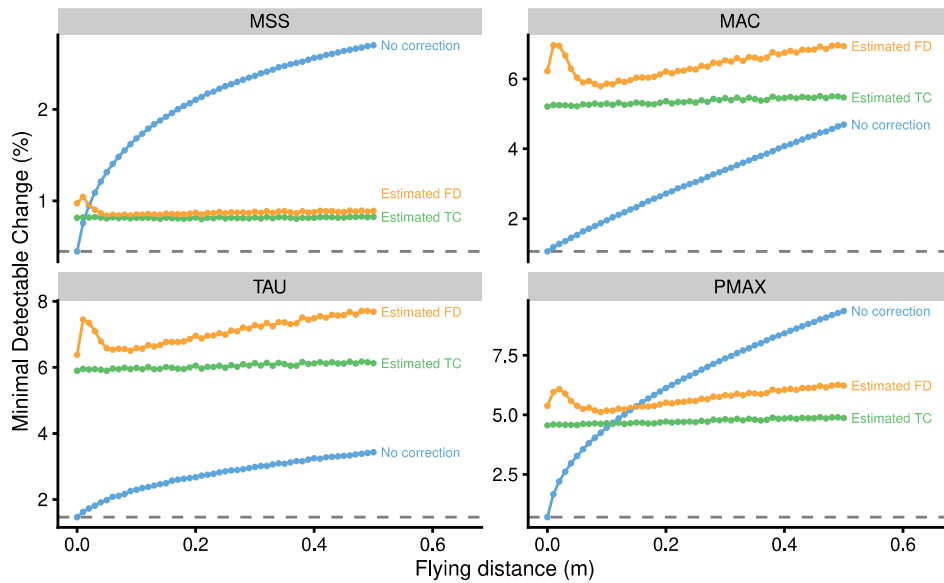
662 *Note.* MSS – maximum sprinting speed; TAU – relative acceleration; MAC – maximum acceleration; PMAX – maximal relative
 663 power



664

665 **Figure 4:** Percentage of the simulations that lie within the region of practical
 666 equivalence (*inside ROPE*) estimated across every flying distance in the simulation for
 667 (1) *No correction*, (2) *Estimated time correction* (Estimated TC), and (3) *Estimated*
 668 *flying start distance* (Estimated FD) models.

669 *Note.* MSS – maximum sprinting speed; TAU – relative acceleration; MAC – maximum acceleration; PMAX – maximal relative
 670 power



671

672 **Figure 5:** Estimated minimal detectable change using 95% confidence level
 673 ($\%MDCs_{95}$) across every flying distance in the simulation for (1) *No correction*, (2)
 674 *Estimated time correction* (Estimated TC), and (3) *Estimated flying start distance*
 675 (Estimated FD) models. The dashed line represents the lowest $\%MDCs_{95}$ estimated
 676 using the *No correction* model and no flying distance ($\%MDCs_{95}^{lowest}$).

677 *Note.* MSS – maximum sprinting speed; TAU – relative acceleration; MAC – maximum acceleration; PMAX – maximal relative
 678 power